

# LOW-MASS TELESCOPE SYSTEMS FOR ASTROPHYSICS AND COMMUNICATIONS APPLICATIONS

MARK DRAGOVAN\*

**Abstract.** A fundamentally new technology for constructing large ( $\sim 10$  to 20 meter aperture), low-mass ( $\sim 1\text{kg}/\text{m}^2$ ) precision reflectors and telescope systems is addressed. The technique is simple: cap a rigid volume with a thin, flat, reflective, and stretchable material (the membrane) then pressurize the volume with a gas, similar to inflating a balloon or soap bubble. The shape of the resulting surface is a good approximation to a conic section with higher order polynomial correction terms. If the membrane is stretched beyond its elastic limit, the shape change is permanent resulting in a freestanding reflective surface after the pressure is released. The shape can be modified by changing the boundary, the pressure, or the membrane material. Using the primary reflector in conjunction with adaptable secondary and tertiary reflectors, wavefront distortion may be corrected, resulting in a diffraction limited telescope system. Measurements of a freestanding membrane suitable for use as a reflector at submillimeter wavelengths are presented.

**1. Introduction.** The history of Astronomy and Astrophysics is in many ways also the history of the telescope and its associated instrumentation. The inspiration for the work described below is both scientific and technical. The scientific motivation comes from two separate branches of astrophysics:  $\gamma$ -ray astrophysics and Cosmic Microwave Background anisotropy experiments. Although having widely different scientific goals, they are united by the common technical need for high quality reflectors of about the same surface precision. Additionally, recent progress in optical communications indicates that large optical collectors will be needed to achieve the data rates necessary for future deep space missions.

The STACEE project<sup>1</sup> is an air Cherenkov experiment designed to measure  $\gamma$ -rays in the previously unobserved region of the spectrum from 20 to 100  $GeV$ . In this region of the high energy spectrum sources such as the Crab pulsar, and active galactic nuclei should be observable. These sources are observed at lower energies ( $<20\text{ GeV}$ ) but *not* at the higher energies ( $>100\text{ GeV}$ ). Investigating where the cutoff occurs enables us to gain insight to the physical processes occurring in these objects.

The Python experiment<sup>2</sup> is designed to observe the anisotropy in the Cosmic Microwave Background (CMB). The fundamental measurement of the angular power spectrum of the fluctuations in the CMB can, within the context of a given model, give very good estimates of the basic constants of cosmology: including the Hubble constant  $H_0$ , and  $\Omega = \rho/\rho_c$ , the parameter determining the geometry of the Universe. The measurements are independent of any of the classical determinations of these constants, providing new insight into the critical constants of cosmology.

The reflectors used for both projects are of modest size ( $<1\text{m}$ ) and surface accuracy ( $8\ \mu\text{m RMS}$ ). The new technology described may be extended to very high quality, low-mass, relatively inexpensive reflectors for telescope systems deployed in Space. The

---

\* Department of Astronomy and Astrophysics and Enrico Fermi Institute, University of Chicago

<sup>1</sup> Ong, R. *Texas Conference on Relativistic Astrophysics 1997*, Chicago II.

<sup>2</sup> M. Dragovan, J. Ruhl, *et al. Ap.J. (letters)* **427**, L67 (1994).

theoretical and experimental issues involved in constructing membrane reflectors are summarized. Current NASA programs that could benefit from this technology are the ARISE space VLBI project, and the OWL airshower detection experiment.

A compelling case can be made for a design that will result in a low-mass, low-emissivity, diffraction limited telescope system. The design is based firmly upon fundamental physical principles, and is scalable to large aperture telescope systems.

**2. Why Large Telescopes?.** Intuitively, one may expect that bigger telescopes are, in some sense, ‘better’. This statement is true for many experiments, but not all. We will quantify how large telescopes are ‘better’, and quantify the other relevant factors that enter into the analysis<sup>3</sup>.

The signal to noise ratio is given by

$$S_N = \frac{St}{\sqrt{(S+B)t}},$$

where  $S$  is the signal, and  $B$  is the background power due to thermal emission, scattered light, and anything else that is not the signal of interest. For any observations we are concerned with,  $B \gg S$ . Rearranging the above expression and solving for  $t$  (the time required to make an observation),

$$t = B_e S_N^2 / S^2.$$

Additionally, we know that the  $S = Aq_e k$ , where  $A = \pi d^2$  is the telescope collecting area,  $q_e$  is the quantum efficiency of the detector, and  $k$  is a constant. Also, note that the correct background to use is  $B_e = q_e B$  because only the *detected* background power is relevant. Hence

$$t = \frac{B_e S_N^2}{A^2 q_e^2 k^2} = \frac{B S_N^2}{\pi d^4 q_e k^2};$$

for  $S_N = 1$  (a detection), we have

$$t = \frac{B}{\pi d^4 q_e k^2}.$$

This remarkable relationship guides us to the relevant factors involved with detection of signals in the presence of a large background. Clearly, minimizing the time to make an observation is a key consideration. Given that  $t \propto d^{-4}$ , a larger aperture is the most important factor. Next comes  $q_e$ , with detector technology advancing this consideration. Finally,  $B$ , the background power, can be reduced by cooling the telescope (in the case of IR observations), or by careful shielding of stray light for optical observations. In

---

<sup>3</sup> Bowen, I.S. *Astronomical Journal* **69**, 816-825 (1964).

Thronson, H.A. *et al. Publications of the Astronomical Society of the Pacific* **107**, 1099-1118 (1995).

the final comparison, a small cooled telescope satisfies a niche that a large ambient temperature telescope cannot fill. Large apertures are advantageous when angular resolution or collecting area (such as with high spectral resolution spectrometers) are important factors.

To cast the above relations in concrete terms, one realizes that a telescope with  $10\times$  greater aperture than any existing will achieve a  $S_N = 1$ ,  $10^4\times$  faster. In other words, a  $100m$  telescope could do in *one hour* what a  $10m$  would take *a year* to accomplish.

### 3. Fundamental Defining properties of a Telescope or Antenna System.

A telescope system<sup>4</sup> is a collection of reflectors<sup>5</sup> that concentrates incoming electromagnetic radiation ('light') to a focal surface. The fidelity of the resultant image and the extent of the focal surface depends upon several key factors:

**3.1. The shapes and surface quality of the reflective elements.** In the ideal world of geometrical optics there exist several solutions to the problem of finding appropriate surfaces that minimize the aberrations over the focal surface. The designs are generally referred to as *aplanatic*. For a two reflector telescope system the Ritchey-Cretien is an example of a Cassegrain configuration; the Gregorian version is known simply as the *aplanatic Gregorian*. Analytic forms for the shapes exist, and so do algorithms to generate the surfaces. A three reflector system can reduce the aberrations further, at the expense of increased complexity. The point is that there exist optimal solutions to the problem<sup>6</sup>. All of the solutions rely upon the optical system satisfying the Abbe sine condition<sup>7</sup>. An algorithm has been developed that generates a corrector system that satisfies the sine condition<sup>8</sup>.

By surface quality we are referring to the RMS deviation of the true surface from the constructed surface. Clearly, the required surface accuracy is dependent upon wavelength, and the Ruze theory<sup>9</sup> quantifies this. The gain of a diffraction limited reflector is given by

$$G = \eta \left( \frac{\pi D}{\lambda} \right)^2 e^{-(4\pi\epsilon/\lambda)^2}$$

where  $\eta$  is the aperture efficiency,  $D$  is the aperture diameter,  $\lambda$  is the wavelength, and  $\epsilon$  is the small scale RMS surface error. For a surface with  $\epsilon = \lambda/28$  the gain is approximately 80% that of a perfect surface; with  $\epsilon = \lambda/75$  the gain is 97% illustrating the need for a high quality reflecting surface. The Ruze theory is valid for random, uncorrelated surface roughness. Non-random errors give rise to a diffraction-grating-like effect, beaming power to the far sidelobes.

---

<sup>4</sup> The term *telescope* will be used as a generic term and applies to communications antennas or light collectors as well.

<sup>5</sup> The terms *reflector* and *mirror* will be used interchangeably throughout the text. However, it is generally the case that the term *mirror* refers to a surface sufficiently smooth that it can be used in the visible region of the spectrum.

<sup>6</sup> see e.g. Wilson, R.N. *Reflecting Telescope Optics I*. Springer, 1996.

<sup>7</sup> see e.g. Luneburg, R.K. *Mathematical Theory of Optics*. University of California Press, 1964.

<sup>8</sup> Dragovan, M., B. Crone, and R. LeHeaney *unpublished*, 1992.

<sup>9</sup> Ruze, J. *Proc IEEE* **54**, 633-40 (1966).

**3.2. The precision to which the individual elements are oriented with respect to one another.** Alignment precision is a practical matter that effects the final performance of the system. An aplanatic design has the largest possible focal surface; misalignment will induce aberrations and reduce the extent of the focal surface. However, since the aplanat's focal surface is larger to begin with, the reduction in the focal surface's extent is less severe as compared to the classical Gregorian.

**3.3. The scattering and diffraction of the incident light due to secondary mirror and supports placed in front of the primary reflector.** The stray, scattered, and diffracted light problem can be divided into several parts: a) scattering from the secondary and its supports b) scattering from the edges of a segmented mirror or the edge of the primary itself c) background emissivity of cracks and from the reflective surface.

**3.4. Requirements.** From the above considerations a set of requirements can be defined that, ideally, a telescope system will satisfy:

- An aplanatic configuration for the telescope design. This gives the largest focal surface that is physically possible.
- Low sensitivity to misalignment. The aplanatic design is forgiving. As a practical matter the support structure can be constructed from low-mass, low-thermal expansion materials.
- Scattering can be greatly reduced, or even eliminated by using an unsegmented, off-axis primary reflector. The only concern then becomes the roughness of the primary surface, its reflectivity, and the edge illumination of the reflectors.
- To minimize the emissivity (or equivalently, maximize the reflectivity) of the surface, the reflective layer must be made of a material with the highest conductivity possible. Silver, copper, or aluminum are all good choices.
- Wavelength independent design. This is not a fundamental requirement, but the telescope system will be more generally useful if it can be used over a broad range of the spectrum. This implies that all reflective optics must be used.

**4. State of the Art Reflectors.** The problem of constructing telescope mirrors has a long history tracing back to Gregory(1663), Newton(1668), and Cassegrain (1672). The first successful glass mirrors with silvered reflecting surfaces were constructed in the late 1850's by von Steinheil in Germany and Foucault in France<sup>10</sup>. The function of any glass or metal mirror is to support a thin film or membrane that actually does the reflecting. To a good approximation this thickness can be determined, for a specific reflecting material, by considering the skin depth

$$\delta = \frac{1}{\sqrt{\pi\nu\mu\sigma_e}}$$

For a very good conductor like copper  $\sigma_e = 5.7 \times 10^7 \Omega^{-1}/m$ ,  $\mu = 1$ ; if we consider a drop in intensity of  $10^6$  to be opaque, we find that the thickness ( $t_r$ ) of the conductive layer is

---

<sup>10</sup> King, H.C. *The History of the Telescope*. Dover, 1979.

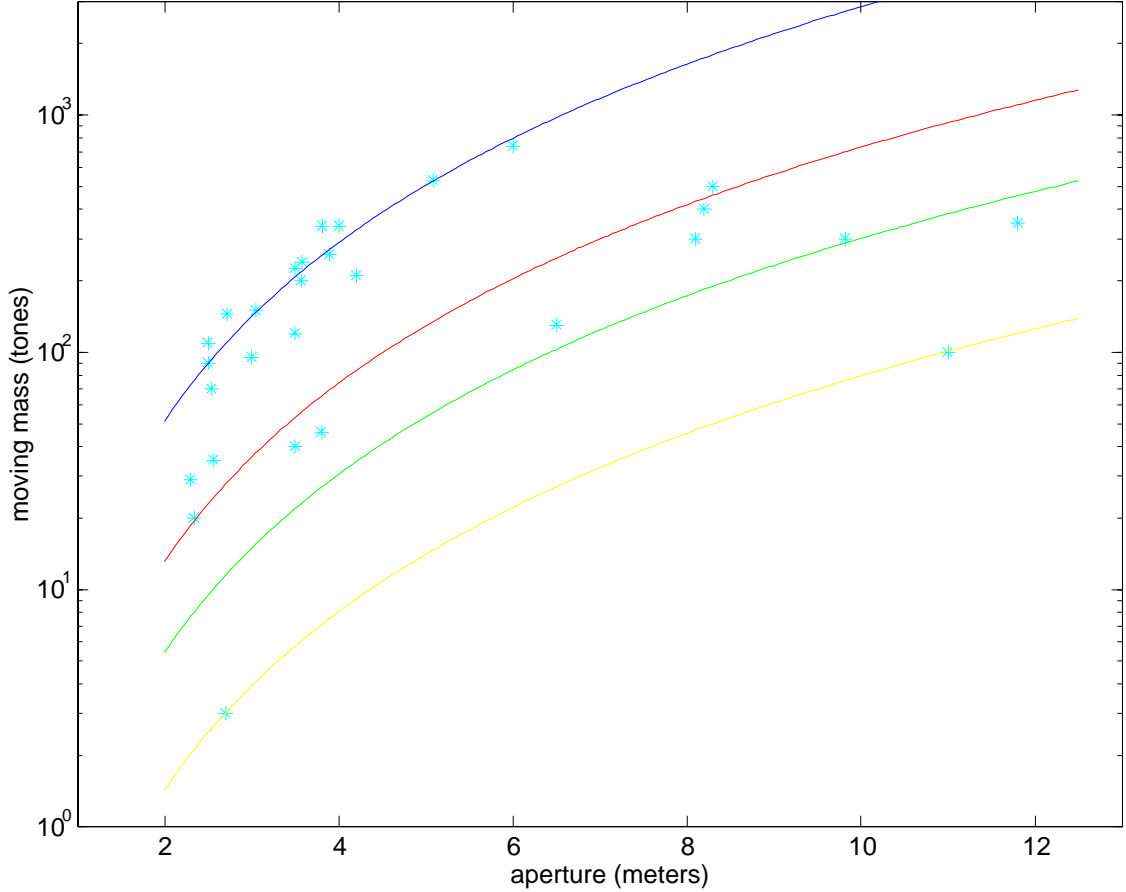


FIG. 1. From top to bottom: 1 the older, thick mirror reflectors, 2 lighter weight thin mirrors, 3 actively controlled surfaces like the Keck, and 4 specialty telescopes with limited general usefulness, but lightweight and designed for a specific purpose.

$t_r = 7\delta$ . In the case of optical light ( $\lambda = 0.5\mu m$ ) the film only has to be 25 nanometers thick to reflect the incident light with little loss; for microwaves ( $\lambda = 1000\mu m$ ) a  $0.85\mu m$  thickness is required. The glass or other backing structure serves only to provide support for this thin reflecting membrane. The areal density of only the reflecting film is given by

$$\begin{aligned} \sigma &= \text{mass/area} = \rho t_r = 7\delta\rho = \frac{7\rho}{\sqrt{\pi\nu\sigma_e}} \\ &\sim 2 \times 10^{-3} g/m^2 = 2 \times 10^{-6} kg/m^2. \end{aligned}$$

This could be considered the theoretical limit on the minimum areal density that is physically possible. Clearly, something is amiss when modern millimetric telescopes have densities of order  $10kg/m^2$ , roughly a factor of  $10^7$  between the reflecting layer and the support structure.

For optical telescopes the situation is much worse. Fig. 1 displays a compilation by the author of the moving mass *vs.* the aperture size for most of the large telescopes constructed to date, including both old and new technology. The telescopes naturally

divide into several distinct regions, with the newer telescopes having lower moving mass. The striking realization one takes away from the plot is that

$$\begin{aligned} \text{mass} &\propto (\text{aperture})^{2.5} \\ \text{or, } \sigma &\propto (\text{aperture})^{0.5}. \end{aligned}$$

This is independent of the technology used, or the epoch when the telescope was constructed. Intuitively one can understand this relationship by realizing that if the diameter were simply increased the mass would scale as the area (i.e.  $\text{mass} \propto (\text{aperture})^2$ ). However, since the stiffness must remain the same, the thickness must also increase. Thus, the exponent must be greater than 2, but not necessarily as large as 3 (which would be the case if the volume were the defining relation).

**5. Beyond State of the Art: Membrane Reflectors.** If there were some way of creating only the desired reflecting surface and not have the heavy supporting structure needed to control the gravitationally induced deformations, the areal density of a reflector could be reduced by several orders of magnitude. For a space based telescope this should be possible, especially if the reflector were constructed in space.

The desired surface may be created by pressurizing a thin metallic membrane beyond its elastic limit. The supporting ring structure is made of a carbon fiber/epoxy composite. The resulting reflector will be near the final correct shape, be very low-mass, and have controllable thermal characteristics. To make a telescope with the membrane reflector requires that the secondary and tertiary optics correct for the aberrations introduced by the primary, on both large and small scales. This is essentially a low-bandwidth adaptive optics system. It is also a fundamentally different way of thinking about telescopes, i.e. a system approach to the design.

The areal density of such a system is straightforward to calculate. For the reflective membrane itself

$$\sigma_m = \rho_m t_r,$$

where  $\rho_m$  is the density of the membrane, and  $t_r$  is its thickness. For the supporting ring

$$\sigma_r = \frac{4\rho_r h(d) \Delta d}{d}$$

where  $\rho_r$  is the density of the ring,  $h(d)$  is the functional dependence of the ring's height on the diameter  $d$  of the ring, and  $\Delta d$  is the width of the ring. The total density is simply the sum

$$\sigma = \sigma_m + \sigma_r = \rho_m t_r + \frac{4\rho_r h(d) \Delta d}{d}.$$

It is instructive to consider two cases,  $h(d) = h$  (a constant height ring), and  $h(d) = h_o(d/d_o)^{1/3}$  (a constant stiffness ring). In the first case the areal density is constant, and

in the latter case actually decreases with aperture. Only if the ring has  $h(d) = h_o(d/d_o)^\alpha$  with  $\alpha > 1$  does  $\sigma$  grow with  $d$ ,

$$\sigma = \rho_m t_r + 4\rho_r h_o (d/d_o)^{\alpha-1} \Delta d.$$

This is in distinct contrast to the data for current mirrors presented in Figure 1, which have  $\sigma = k d^{0.5}$ . Thus, not only is a membrane reflector less massive to begin with, but the areal density can actually *decrease* with larger apertures.

**6. The Shape of a Pressurized Membrane.** A pressurized membrane takes on a shape that minimizes the total energy of the system consisting of the membrane, the gas and the structure rigidly holding the membrane. There are three distinct shapes that can form, depending upon how the tension,  $\gamma$ , in the membrane distributes itself. Soap films, elastically deformed membranes, and plastically deformed membranes are discussed.

Soap films take on shapes that minimize the energy of the film. Since the energy of the film is proportional to the surface area, the question of finding the minimal energy surface reduces to finding the surface of minimal area satisfying the boundary conditions. The problem of finding minimal surfaces is known as Plateau's problem, after the Belgian physicist Joseph Plateau (1801-83), who studied the problem using soap films<sup>11</sup>.

By choosing the appropriate curve for the boundary and pressurizing the film so that it bulges out from the frame, convex or concave surfaces can be formed. In the simplest incarnation the boundary can be chosen so that the film is a segment of a torus, with the degenerate case being a circular boundary which yields a spherical surface. This is interesting because a segment of any surface with non-zero mean curvature can be approximated to some degree by a torus (a surface that has two radii of curvature). An off-axis segment of an ellipse or parabola can be fit quite well by a torus.

The surface tension,  $\gamma$ , is measured in units of [force]/[length] and is the proportionality constant between the energy in the membrane and the area of the surface. Thus,

$$E = \gamma A.$$

The energy of the membrane is given by:

$$E = \gamma \iint_S \sqrt{1 + |\nabla u|^2} dA$$

where  $u(x, y)$  is the function representing the surface, and the integral being taken over the surface  $S$ .

If the tension is uniform across the membrane, then the problem of finding the minimum energy reduces to finding the minimal surface satisfying the boundary conditions. Applying the Euler-Lagrange equations to the above integral gives

---

<sup>11</sup> see e.g. Almgren, F.J. *Plateau's Problem*. Benjamin, 1969; or Isenberg, C. *The Science of Soap Films and Soap Bubbles*. Dover, 1992.

$$\nabla \cdot \left( \frac{\nabla u}{\sqrt{1 + |\nabla u|^2}} \right) = k,$$

where  $k$  is proportional to the pressure difference across the membrane. In fact

$$k = p/2\gamma = \left( \frac{1}{r_1} + \frac{1}{r_2} \right),$$

where  $r_1$  and  $r_2$  are the two radii of curvature of the surface<sup>12</sup>.

The soap film is a very special case of a membrane where the material is perfectly elastic, and can redistribute itself so that the tension  $\gamma$  is everywhere constant. Next is a rigid membrane that remains elastic, but has considerable deformation. Here  $\gamma(r, \theta)$ , is *not* constant as can easily be seen by noting that at the boundary, where the membrane is clamped, the tension is fixed; however, in the free radial direction the tension can change (i.e.  $\gamma(r, \theta) = \gamma(r)$ ). The third case is that of plastic deformation. Again  $\gamma(r, \theta)$  is not constant, but when the pressure is released, the membrane *does not* return to its original state. This is the situation we are in with membrane reflectors. A variational analysis can be performed for the elastic and plastic flow cases<sup>13</sup>, with the result being that the shape of the membrane is well approximated as a conic section with higher order polynomial deviations. Measurements are discussed next.

**7. Measuring the Membrane Shape and Roughness.** Given that the membrane is only 50  $\mu m$  thick, a non-contacting sensor is needed so that the process of measuring the profile of the surface does not distort the surface. We are using a non-contacting laser displacement meter. The resolution of the device is 30  $nm$ , with a reproducibility of 3  $\mu m$  with our current setup. The limitation at present is that there is a vibration that is contaminating the results; we are in the process of eliminating this source of error.

The shape of the membrane is taken to be a conic section with additional higher order polynomial terms. The analytic form of a conic is

$$z(r) = \frac{cr^2}{1 + \sqrt{1 - sc^2r^2}} + \sum_{i=0}^n a_i x^i.$$

This form is appropriate if the boundary is circularly symmetric. If the boundary is not circularly symmetric, or one wants to do a fit to see how symmetric the surface is, the form used is called a biconic and has the form

$$z(r) = \frac{c_x x^2 + c_y y^2}{1 + \sqrt{1 - s_x c_x^2 x^2 - s_y c_y^2 y^2}} + \sum_{i,j=0}^n a_{ij} x^i y^j.$$

It is clear by inspection that a biconic reduces to a symmetric conic if  $c_x = c_y$ , and  $s_x = s_y$ .

<sup>12</sup> see e.g. Struik, D.J. *Lectures on Classical Differential Geometry*. Dover 1988.

<sup>13</sup> Murphy, L.M. *Journal of Solar Energy Engineering* **109**, 111-120 (1987).

Weil, N.A. and Newmark, N.M. *Journal of Applied Mechanics*, pp 533-538 Dec (1955).

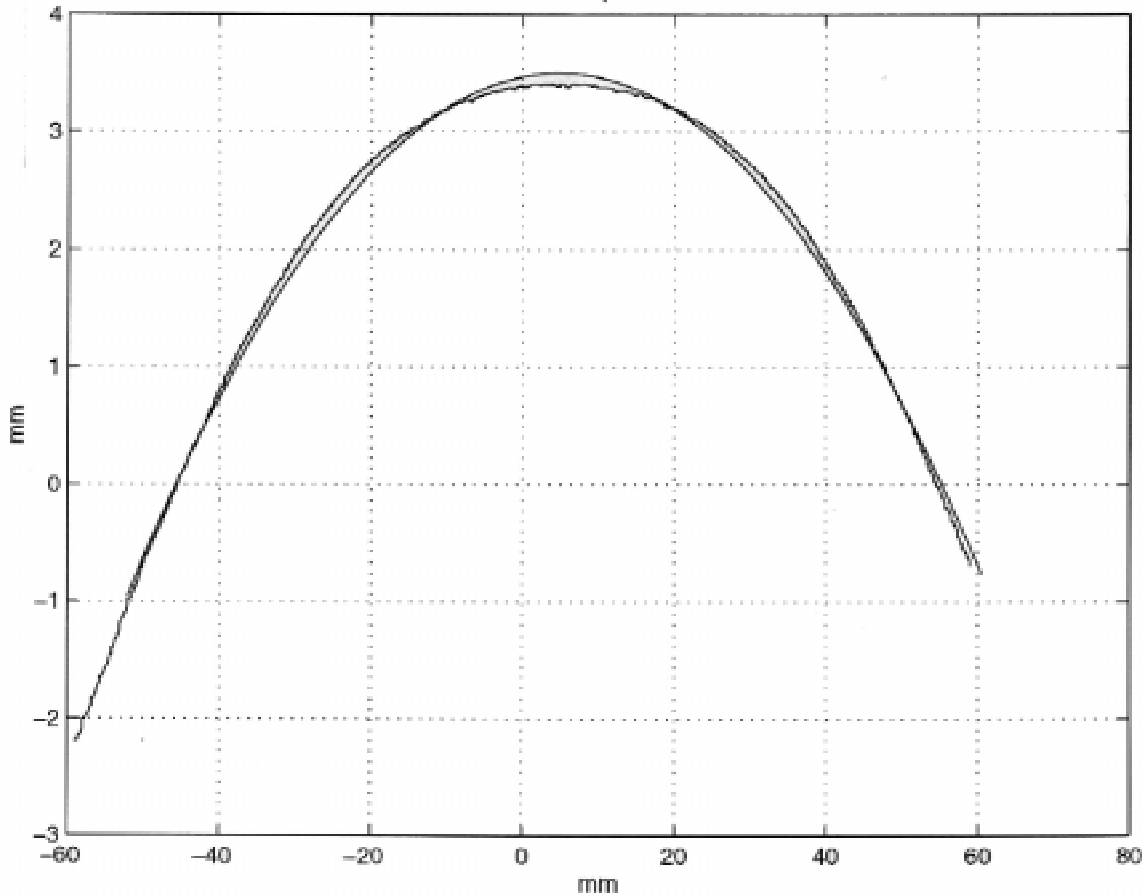


FIG. 2. *Surface measurements with a parabolic fit overlaid. The units on both axes are mm. One should note that the measured data are flatter in the center than the parabolic fit indicating the surface is closer to spherical in the center region. If the surface tension were uniform throughout the membrane (as in a soap bubble) the surface would be spherical.*

**8. Results.** For the 50 cm (20") diameter, 50  $\mu\text{m}$  thick membrane reflector we fit the measured data to a parabolic surface obtaining the following fit parameters (using the standard form for a symmetric conic):

$$c = -0.002734$$

$$s = -1.000$$

with additional 8th order polynomial terms. Plots of the data and fits are presented below.

Figure 2 is a plot of the data with the parabolic fit overlaid. By inspection one can see that the fit and the data overlap, but there are deviations from a true parabolic section. Figure 3 is a plot of the deviations between the data and the parabolic fit. By examining the figure it is clear that the deviations can be described by a polynomial. When the polynomial is fit, the residuals form a Gaussian distribution (indicating that the global fit is quite good and the standard deviation is a good estimate of the uncertainty in the measurement, Figure 4). The fit gives an RMS of  $8\mu$  over the central

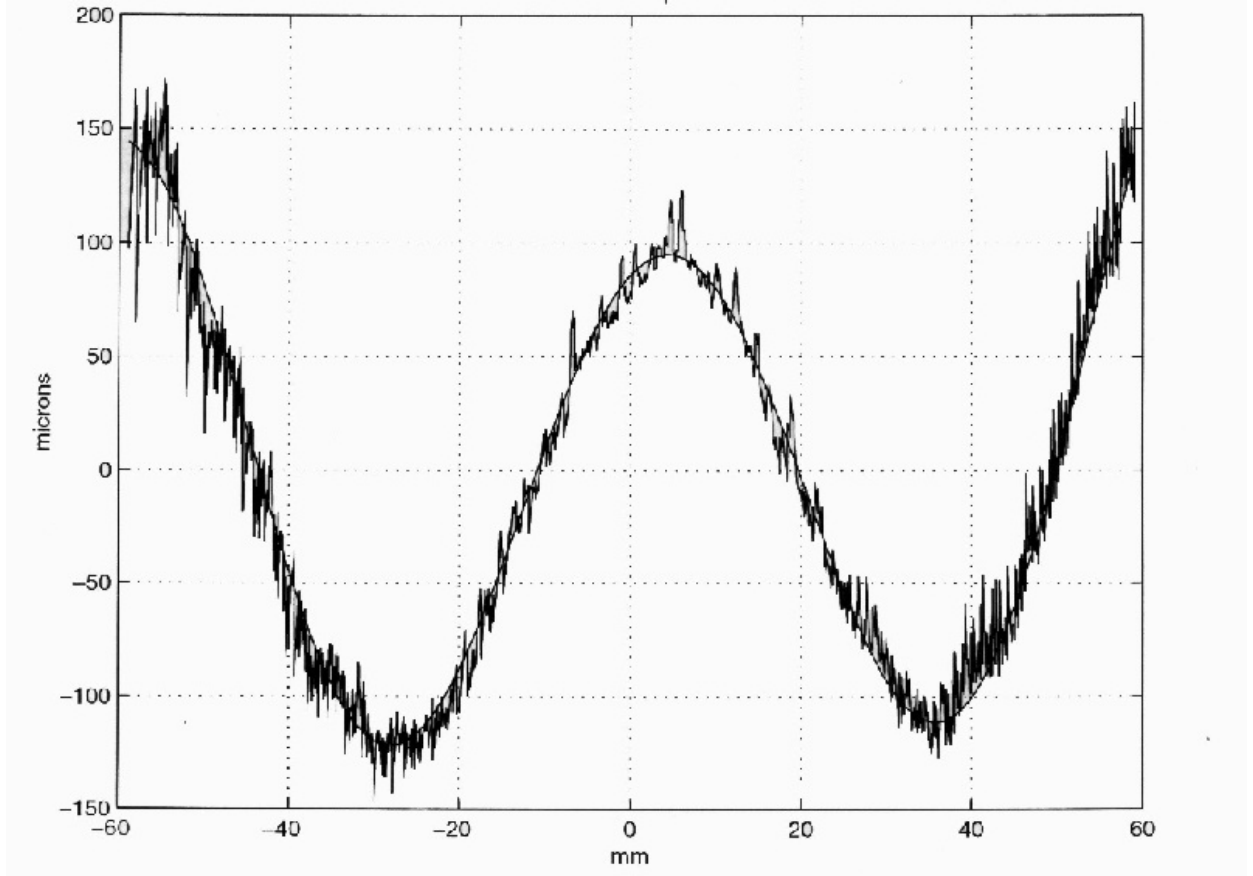


FIG. 3. The residuals of the difference between the measured data and the parabolic fit. The units of the ordinate are microns, and the abscissa are millimeters. For use as a submillimeter reflector operating at  $\lambda = 200\mu\text{m}$  this corresponds to a wavefront distortion of only  $\pm 1\lambda$ .

120mm of the reflector. The salient features of the membrane reflector described in this section are summarized in table 1.

By inspection of Figure 2 it is clear that the center is flatter than the edges indicating the shape is closer to spherical than parabolic. This is to be expected as the center is the region that has the greatest amount of stretching as compared to the edge. A parabolic fit was used in order to estimate the total wavefront error that must be corrected to bring the system to a focus. For use as the primary reflector of a submillimeter telescope operating at  $\lambda \gtrsim 200\mu\text{m}$  the beam efficiency will be  $\sim 80\%$  after correcting the  $\sim \pm 1\lambda$  surface shape error.

| Table1                     |  |
|----------------------------|--|
| material                   | type 321 Stainless Steel   |
| size                       | 50 cm diameter, $50\mu\text{m}$ thick                            |
| surface shape<br>curvature | parabolic ( $s = 1$ ) with higher order terms<br>$C = -.0027344$ |
| surface roughness          | $8\mu\text{m}RMS$  |

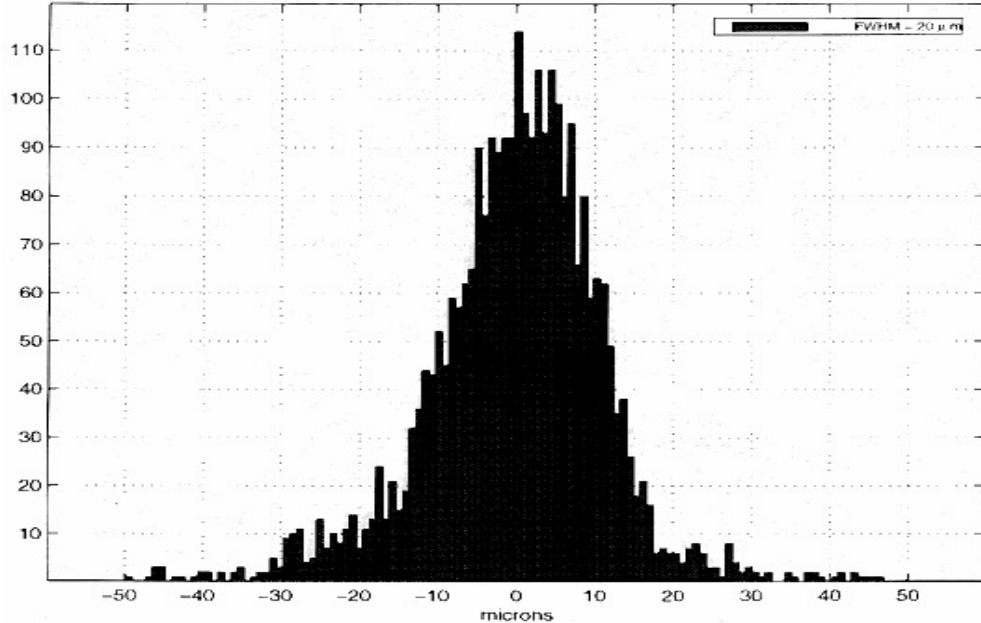


FIG. 4. Histogram of the residuals after fitting the surface with a parabolic conic section and an 8th order polynomial. The Gaussian form of the distribution indicates the goodness of fit. The FWHM is 20  $\mu\text{m}$ .

**9. Optical Design.** The optical system consists of the primary, secondary, and tertiary reflectors in a Gregorian Configuration. The secondary and tertiary reflectors form an adaptable wavefront correction system. The tertiary is located at a position which is an image of the primary. For the example presented in figures 5 and 6 the magnification is approximately 5; thus the primary appears to be about  $5\times$  smaller at the location of the tertiary. A small bump on the primary is imaged onto the tertiary, the tertiary may be deformed at that point to correct for the bump. Thus a global wavefront error induced by the membrane reflector is removable by deforming the tertiary appropriately. The resulting telescope system can be diffraction limited. The surfaces can be designed to satisfy the Abbe sine condition, consequently the system will have a reasonable field of view.

Ray traces of the optical system are presented in Figures 5 and 6. This is an off-axis configuration that serves as the basis of the optical design. The secondary images the primary onto the tertiary. The system meets all the requirements addressed in section 3. The design has elements in common with a 2 meter millimetric telescope designed by the author for studying low-contrast astrophysical sources such as the Cosmic Microwave

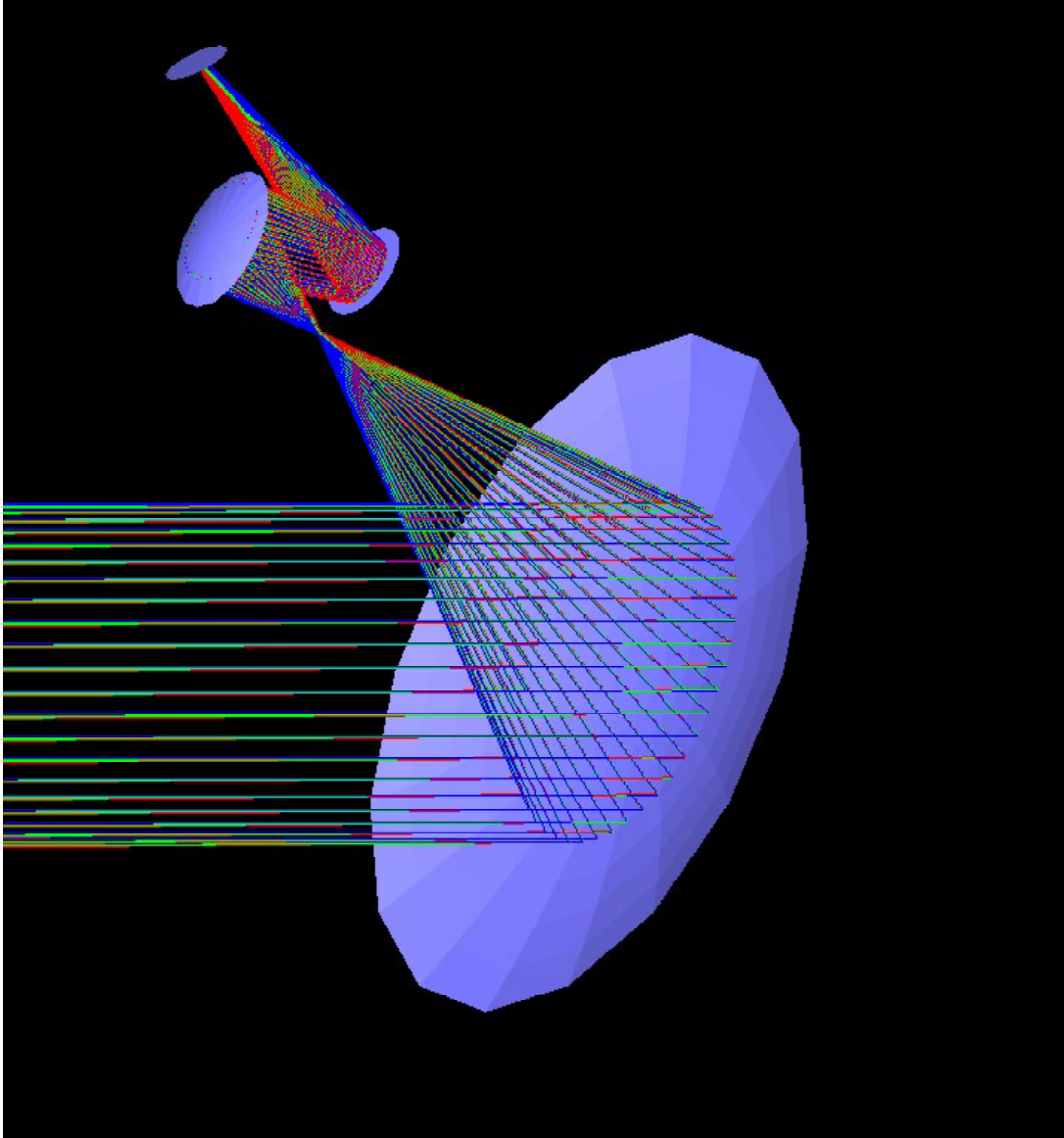


FIG. 5. A perspective view of the off-axis Gregorian telescope system. The primary is a low-mass membrane reflector. The secondary and tertiary reflectors form an adaptable wavefront correction system.

Background Anisotropy<sup>14</sup>.

**10. A Large Aperture Space Telescope.** The concept is simple: Launch a large piece of thin foil that has been rolled up (much like the aluminum foil rolls one can buy at any convenience store) along with its supporting/stretching ring structure into orbit. Assemble the pieces (i.e. unroll the foil sheet, clamp the membranes in the stretching jig), and inflate the membranes. In order to minimize the mass there will

---

<sup>14</sup> Preliminary scientific results were presented at the ‘Texas’ meeting held in Paris, France in December 1998. A short report appears in the Jan 1, 1999 issue of *Science*.

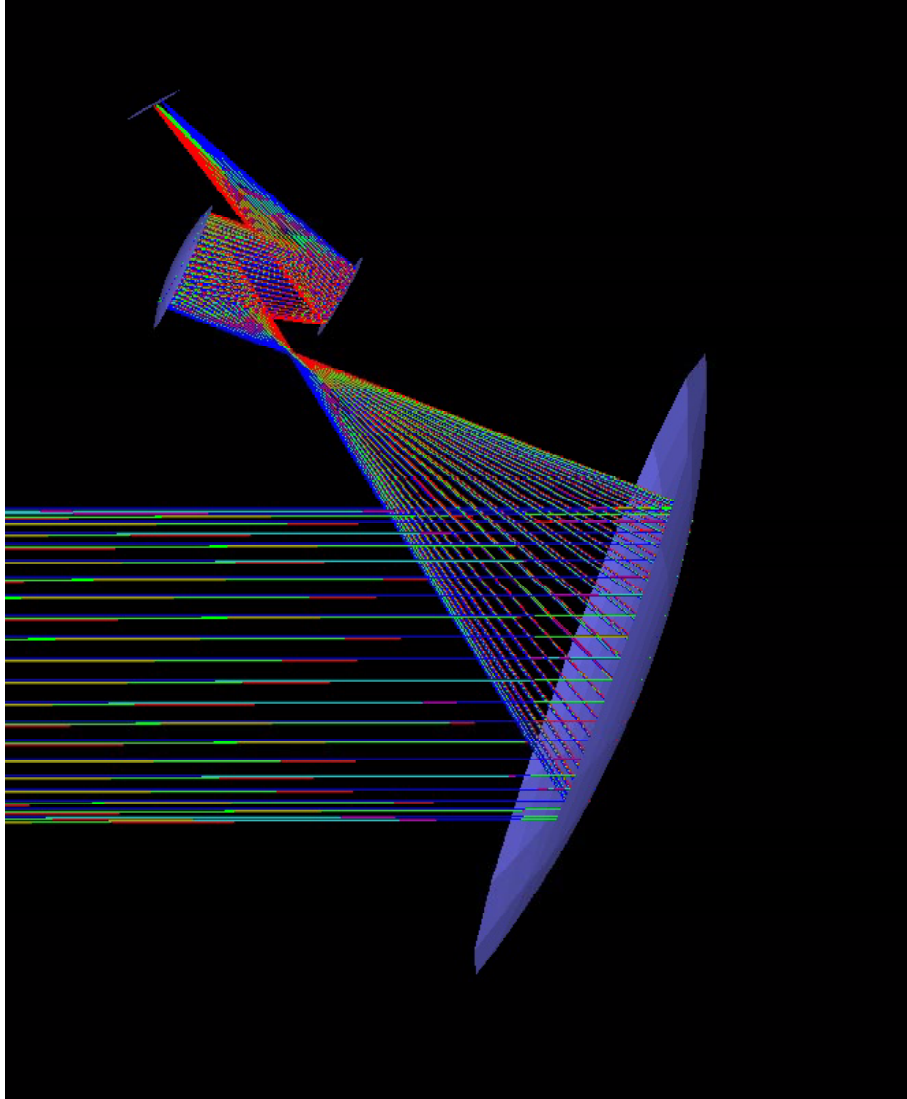


FIG. 6. Side view illustrating the reimaging of the primary. The secondary produces an image of the primary at the location of the tertiary.

be two membranes stretched, one can be used for the reflecting mirror, and the other for the sun or meteoroid shield. Figure 7 shows the assembly concept, while Figure 8 shows what the inflated membranes will look like.

After the reflectors are formed they are assembled into a telescope system as illustrated in Figures 5 and 6. The system is tuned by observing a bright point source. The adaptable optics are adjusted until an optimal image is obtained.

**11. Summary.** The classical telescope mirror is clearly an object of wonder: a device that evolved over the past few centuries from apertures of a few inches in diameter in Newton's time, to the 10 meter behemoths that will populate several of the Earth's mountain tops today. Upon reflection, one realizes that all this mass is used to support only a thin film of metal a few hundred nanometers thick. Comparing the mass of the

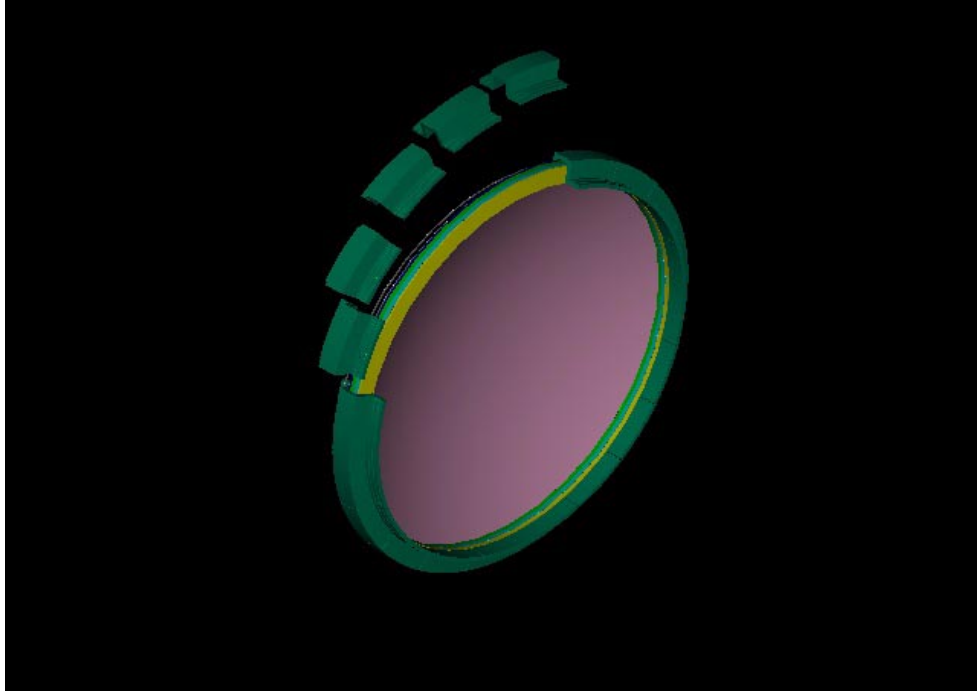


FIG. 7. *The membrane and supporting ring, showing how the support structure is assembled.. The support ring is composed of a number of smaller sections that serve to keep pressure on the membrane and prevent it from slipping.*

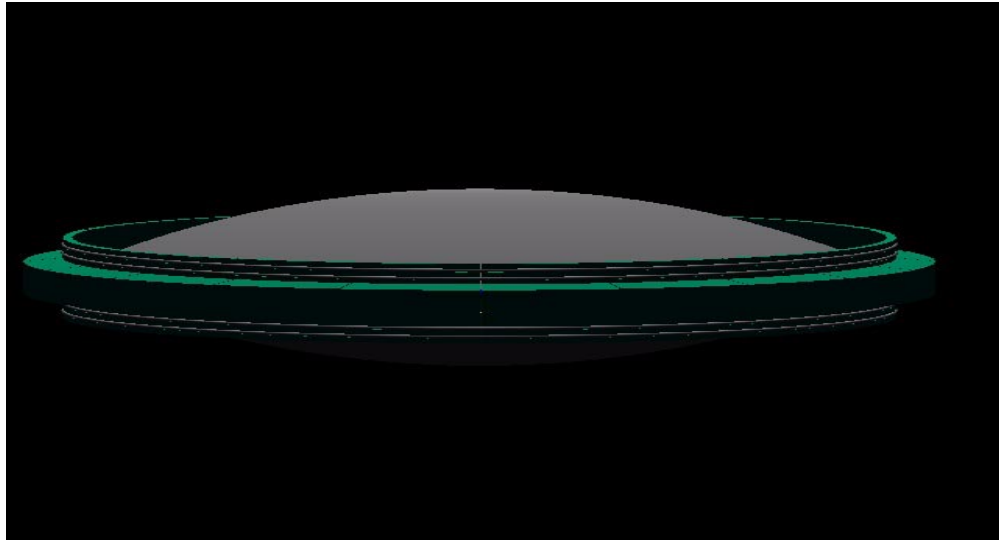


FIG. 8. *The final reflector after pressurizing. The lenticular structure is due to the forming process using two membranes, and a single boundary ring. Gas is introduced into the region between the two membranes, pressurizing the membranes and stretching them beyond their elastic limit. After forming the pressure is released, and two self supporting membranes remain. One can be used as a shield for the primary reflector.*

reflective film to that of the backing structure one finds that something clearly is amiss, and a re-examination of the fundamentals of mirror fabrication and telescope design are in order.

The concept of the telescope as a system rather than as a collection of very precise individual mirrors and re-examining mirror fabrication techniques are the basis of a new class of large, low-mass telescopes. The basic idea is to construct the primary mirror (the largest most massive surface) with the least precision, putting the effort of correcting the defects of the primary with the secondary and tertiary optics. The primary reflector is produced with a novel technology, that of plastically deforming a reflective membrane. A reflector usable at submillimeter wavelengths has been produced. Larger, higher quality mirrors are under development.

**12. Acknowledgments.** I wish to thank G.H. Marion and A.K. George for assistance with the construction and characterization of the membrane mirrors. Careful reading of the text by K. Coble, G.H. Marion, and J. Kovac improved the presentation. This work has been supported by the NSF, NASA, and the Fullam Award of the Dudley Observatory.